# Lattice dynamics of the superionic conductor AgI†

Richard Alben*
*Department of Engineering and Applied Science, Yale University, New Haven, Connecticut 06520*

Gerald Burns
*IBM Thomas J. Watson Research Center, Yorktown Heights, New York 10598*

(Received 22 June 1977)

We present results of harmonic lattice-dynamics calculations of the density of states, infrared conductivity, and Raman scattering for the superionic conductor AgI. The calculations do not incorporate the low-frequency, diffusive aspects of the ionic motion, but they do contain the oscillatory aspects in some detail. We find that the intrinsic disorder of the $\alpha$ phase accounts for the broad spectra which are observed. In particular, the density of states and the calculated spectra display a lower-frequency transverse-acoustic-like feature as well as an upper-optic-mode peak at $\approx$ 100 $cm^{-1}$ in agreement with experiment. We also consider effects of possible defect sites on the spectra of the wurtzite and $\alpha$ phases of AgI.

## I. INTRODUCTION

Silver iodide is a superionic conductor,[1] perhaps the classical material of this type. It has the wurtzite crystal structure ($C_{6v}^4 - P6_3mc$) below $T_c$ = 147°C and the defect "$\alpha$-phase" crystal structure ($O_h^9 - Im3m$) above. At $T_c$ there is an increase of a factor $10^4$ in the dc conductivity, to about 1.3 $(\Omega\, cm)^{-1}$, making $\alpha$-phase AgI one of the best superionic conductors known.

Our calculations give standard harmonic lattice-dynamics solutions for the density of states and the first-order infrared and Raman response. We make no effort to incorporate the effects of diffusive motion which dominate the spectra below 10 $cm^{-1}$. However, the disordered nature of the material is taken into account in a fairly sophisticated manner. The results are compared to experiment, and it is found that many spectral features can be accounted for by these calculations. A preliminary account of this work has been given.[2]

## II. DESCRIPTION OF THE CALCULATIONS

There are four ingredients that go into our calculations of vibrational spectra: (a) a model for the equilibrium atomic positions, (b) a model for the interatomic forces, (c) expressions for the changes in polarizability and dipole moment associated with atomic displacements, and (d) a method for efficiently solving the harmonic lattice-dynamics problem for systems with finite but large numbers of degrees of freedom. We discuss each of these in turn.

### A. Models

In our calculations, each crystal structure is approximated by finite clusters of 1000-2000 atoms with periodic boundary conditions. The clusters are rectangular, containing about 250 unit cells of the different crystal structures.

Figure 1 shows a unit cell of $\alpha$-phase AgI proposed by Strock[3] in 1934. He found that the $I^-$ ions are on the two $a$ sites of the $Im3m - O_h^9$ space group. These are the body-centered sites, as can be seen in the figure. To solve the structure, he distributed the $Ag^+$ ions uniformly on the 6 $b$ sites (6-neighbor, octrahedral environment), 12 $d$ sites (4-neighbor, tetrahedral environment), and 24 $h$ sites (5-neighbor, trigonal bipyramidal environment), making a total of 42 sites for the two $Ag^+$ ions. From crystal chemical thinking[4] and interpretation

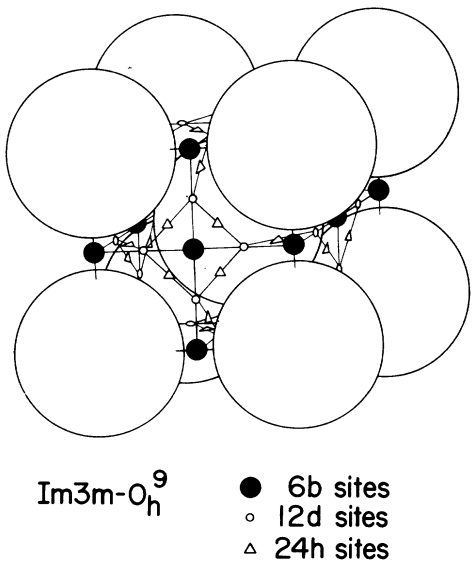


FIG. 1. High-temperature $\alpha$ phase of AgI. The large circles are the $I^-$ ions and the possible sites of $Ag^+$ are shown.

of the spectra[5] it has been suggested that only the 12 $d$ sites are appreciably occupied. This has been confirmed by more recent x-ray,[6] EXAFS[7] (extended x-ray absorption fine structure), and neutron[8] work. Thus, we model $\alpha$-phase AgI with the $Ag^+$ ions randomly distributed on the 12 $d$ sites. However, the choice of sites is further restricted, so that once a given $d$ site is filled, its four nearest-neighbor $d$ sites are excluded. In some of our calculations for the $\alpha$-phase we have also allowed small displacements of each $Ag^+$ ion toward one of its neighboring $d$ sites. Such displacements are experimentally observed.[7,8]

For perfect wurtzite AgI, we take ideal $c/a$ and internal displacement parameters. We also consider wurtzite AgI models with a displacement of each $Ag^+$ toward one of the faces of the tetrahedron formed by its neighbors. This has been reported in some x-ray work by Helmholtz, although other researches have not agreed.[9] However, this type of displacement appears to occur clearly in CuI-type superionic conductors.[10] The long-wavelength optic modes in perfect wurtzite transform as the $A_1+2B_1+E_1+2E_2$ irreducible representations of the $C_{6v}-6mm$ point group. From low-temperature polarized Raman measurements,[11] the frequencies of the $A_1(\mathrm{TO})+A_1(\mathrm{LO})+E_1(\mathrm{TO})+E_1(\mathrm{LO})+2E_2$ modes have been determined, where TO and LO mean the transverse- and longitudinal-optic modes, respectively. Some of these mode frequencies are used, as discussed in the next section, to determine the parameters in the interaction potential.

### B. Interaction potential

We describe the interatomic interactions by a simple potential which is second order in the displacements $\vec{u}$ of the atoms from their equilibrium positions and includes only nearest-neighbor AgI forces[12]:

$$V=\frac{1}{2}\sum_{\langle i,j\rangle}\{\alpha'_{ij}[(\vec{u}_i-\vec{u}_j)\cdot\hat{r}_{ij}]^2+\beta'_{ij}(\vec{u}_i-\vec{u}_j)^2\}, \quad (1)$$

where the sum is over all pairs of nearest neighbors[13] and $\hat{r}_{ij}$ is the unit vector between neighbors. There is a central force of magnitude $\alpha'+\beta'$ and a noncentral force of magnitude $\beta'$. For the perfect wurtzite model, the parameters $\alpha'$ and $\beta'$ are chosen to fit the observed[10] $E_2$ mode at 17 $\mathrm{cm}^{-1}$ and the weighted-average frequency of 112 $\mathrm{cm}^{-1}$ of the $A_1$ and $E_1$ TO and LO modes. This gives $\alpha'=29.57\ N/m$ and $\beta'/\alpha'=0.035$.

Although we have left out important interactions, such as the long-range Coulomb effects, the simple potential approximately reproduces the dispersion curves observed by neutron scattering in wurtzite AgI at low temperature.[14] For $\alpha$-phase AgI with $Ag^+$ ions occupying the tetrahedral 12 $d$ sites, we use the same potential with the same values of $\alpha'$ and $\beta'$ as for the wurtzite phase. Thus, there are *no new parameters introduced* for the $\alpha$ phase. For models with $Ag^+$ ions displaced from the tetrahedral positions, we allow $\alpha'$ and $\beta'$ to vary somewhat, depending on the separation of different types of near-neighbor pairs.

### C. Displacement-dependent dipole moment and polarizability

The atomic motions in a material give rise to infrared and Raman spectra via the time-dependent variation of the dipole moment and the polarizability, respectively. We confine our attention to first-order spectra for which only terms linear in the displacements are required.

For the dipole moment, the most general form is

$$\vec{P}=\sum_i \vec{B}_i\vec{u}_i, \quad (2)$$

where the sum is over all atoms. In a disordered material, the $\vec{B}_i$'s will, in principle, depend on the kind of atom and on its local and even distant environment. We take the simplest form allowed by symmetry which gives a nonzero effect:

$$\vec{B}=\pm e\vec{I}, \quad (3)$$

where $e$ is the electronic charge, $\vec{I}$ is the unit tensor, and $\pm$ applies to $Ag^+$ and $I^-$ ions, respectively.

For first-order Raman scattering, we need an expression for the linear change of polarizability $\vec{A}$ with atomic displacements. The general form, for the $\gamma\beta$ element of the $A$ tensor, is

$$A^{\gamma\beta}=\sum_{i,\alpha} D_{i\alpha}^{\gamma\beta}u_{i\alpha}, \quad (4)$$

where the sum on $i$ runs over all atoms, the sum on $\alpha$ runs over the $x$, $y$, and $z$ directions, and the third-rank tensors $D_i$ depend on atom $i$ and its neighbor environment. The simplest form for the $D$'s is one which involves only the nearest-neighbor unit vectors for each atom and requires three parameters.[13,15] They are denoted by $d_1, d_2$, and $d_3$ in the expression

$$d_{i\alpha}^{\gamma\beta}=\sum_j{}'[d_1(\hat{r}_{ij}^{\gamma}\hat{r}_{ij}^{\beta}-\tfrac{1}{3}\delta_{\gamma\beta})\hat{r}_{ij}^{\alpha} + d_2(\tfrac{1}{2}\delta_{\alpha\gamma}\hat{r}_{ij}^{\beta}+\tfrac{1}{2}\delta_{\alpha\beta}\hat{r}_{ij}^{\gamma}-\hat{r}_{ij}^{\gamma}\hat{r}_{ij}^{\beta}\hat{r}_{ij}^{\alpha}) + d_3\delta_{\gamma\beta}\hat{r}_{ij}^{\alpha}].$$

The primed sum runs over the nearest neighbors of atom $i$, and $\hat{r}_{ij}^{\alpha}$ is the projection of the $\hat{r}_{ij}$ unit vector on the $\alpha$ direction. The $d_1$ parameter measures the depolarized scattering due to bond stretching, the $d_2$ parameter measures the depolarized scattering due to bond rotation, and the $d_3$ parameter

measures the polarized scattering due to bond stretching. We have no *a priori* way of setting the $d$ parameters. For purposes of illustrating the results, we have computed the scattering for three cases with each $d$ in turn set equal to unity while the other two are zero. The light polarizations are taken in the skew, $\langle 111 \rangle$, direction to roughly mimic a powder spectrum. (Polarizations in several directions give similar results.) We display the results for each $d$ separately. The results are then added together, with twice the weight given to the polarized as the depolarized spectra. The latter choice is dictated by the experimental observation that polarized scattering predominates in the disordered materials.[16,17]

We note at this point that the Raman intensity calculated from Eq. (5) is the "reduced" Raman intensity, and when we compare to experimental results, we always plot the reduced Raman intensity. Thus, if one obtains an experimental Stokes intensity $I_R$, which is naturally a function of temperature and frequency, what we call the Raman spectra is

$$\omega I_R/(1+n), \tag{6}$$

where $n$ is the Bose-Einstein factor $[\exp(\hbar\omega/kT)-1]^{-1}$.

In contrast to the force-constant model, which we believe is adequate as a first approximation, the models for the couplings of atom displacements to optical processes can only be considered a crude description of the complex processes in a real material. Still, we believe that there is much to be learned from these calculations of spectra based on coherently added contributions from the displacements of individual atoms. For the perfect-crystal wurtzite models, as will be seen, this approach picks out the handful of allowed modes from the thousands of modes which make up the density of states for the models. For the $\alpha$-phase and disordered wurtzite models there are no strict selection rules, but there are effects of local symmetries in determining the relative intensities in different parts of the spectra. In particular, for acoustic-like modes, where neighboring atoms tend to move in the same direction, the individual contributions in Eqs. (2) and (4) largely cancel, so that long-wavelength modes have relatively weak couplings as expected from hydrodynamic considerations.

### D. Methods of calculation

The usual way of solving a harmonic lattice-dynamics problem is matrix diagonalization.[15,18] However, with systems of several thousand degrees of freedom, matrix methods become quite inefficient. We have thus chosen to use the "equation of motion" method.[13] This gives results which are equivalent to the usual analysis, except that the spectra are naturally broadened by a Gaussian. We choose the width of the broadening function to be narrower than the true features which we expect for disordered systems, but broad enough to smooth out variations in the spectra due to the finite size of the cluster. We used a broadening of about 5 $cm^{-1}$ in most of the calculations. For comparisons with experiment, we use a 15-$cm^{-1}$ width to reduce the distracting fine scale structure.

## III. RESULTS FOR WURTZITE AND $\alpha$-PHASE AgI

Experimentally, in the wurtzite phase, the $A_1$ and $E_1$ TO modes are degenerate and occur at 106 $cm^{-1}$. Similarly, the $A_1$ and $E_1$ LO modes are degenerate at 124 $cm^{-1}$. These modes are all ir active. For the Raman spectra these modes as well as two $E_2$ modes, which occur at 17 $cm^{-1}$ and 112 $cm^{-1}$, are active. Because of the neglect of long-range Coumb forces in the calculation, we do not obtain an LO-TO splitting at the zone center, and obtain $\alpha'$ and $\beta'$ in Eq. (1) by fitting the "average" position of the $A_1$ and $E_1$ modes at $\frac{1}{3}(2\text{TO}+1\text{LO}) = 112$ $cm^{-1}$ and the 17-$cm^{-1}$ $E_2$ mode as mentioned before.

The results of calculations for the wurtzite phase are shown in Fig. 2. The density of states has two

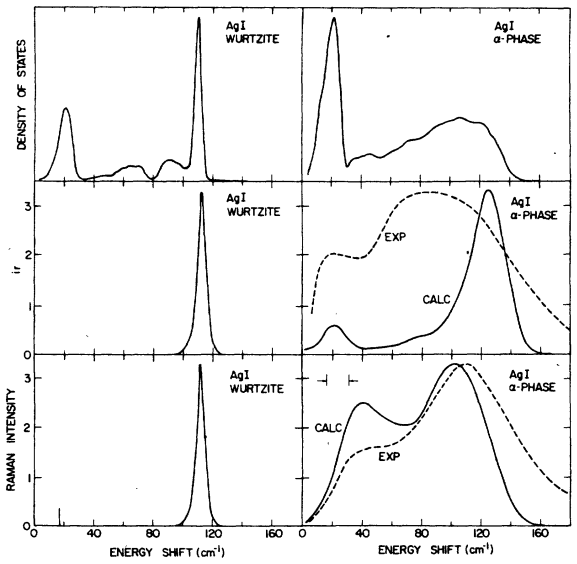


FIG. 2. Calculated density of states, infrared conductivity, and Raman spectra (solid lines) for perfect wurtzite AgI and perfect $\alpha$-phase AgI. Experimental results (dashed lines) are also shown. The resolution is 5 $cm^{-1}$ for the three wurtzite calculations and $\alpha$-phase density-of-states calculation and 15 $cm^{-1}$ (shown on the bottom right) for the ir and Raman $\alpha$-phase calculations as discussed in the text. The vertical line at 17 $cm^{-1}$ for wurtzite Raman results shows the position of the $E_2$ mode whose calculated intensity ($10^{-5}$ of the upper modes) is too weak to be shown directly.

major and two minor peaks as is usual for tetrahedrally bonded systems. A "mass separation" of the acoustic and optic branches almost occurs at $\approx 80$ $cm^{-1}$. For a larger mass difference between the positive and negative ions this mass separation becomes much more pronounced. The peak at low frequency comes from TA (transverse acoustic) modes which entail bending of bonds but little or no bond stretching. Fully one-third of the modes are of this type. The infrared and Raman spectra are weighted superpositions of the allowed modes. For ir, the allowed modes $A_1$ and $E_1$ are degenerate because of the ideal crystal parameters and the neglect of Coulomb forces. The calculated ir response, shown in Fig. 2 at 112 $cm^{-1}$, has a half-width of 5 $cm^{-1}$, which is the resolution of the calculation. No other ir response occurs in the calculation, in agreement with experiment.[19] The results of the Raman calculation are also shown in Fig. 2. We do not resolve the $A_1$ and $E_1$ modes from the upper $E_2$ mode. This agrees with experiment, since the average $A_1$ and $E_1$ mode occurs at 112 $cm^{-1}$, as does the upper $E_2$ mode. The lower-frequency $E_2$ is so weak for our calculation ($\sim 10^{-5}$ of the intensity of the upper-frequency $E_2$ mode) that it cannot be shown to scale, and it is indicated by the vertical line at 17 $cm^{-1}$. Again, note that the mode at 112 $cm^{-1}$ is 5 $cm^{-1}$ wide, which is the resolution of the calculation.

The results of the calculations for the $\alpha$ phase are shown on the right side of Fig. 2, and they may be compared to the results in the perfect wurtzite structure. The density of states for the $\alpha$ phase shows some similarity to that for the wurtzite phase. Again there are a large number of low-frequency modes as expected for approximate tetrahedral bonding. (Recall that $Ag^+$ ions in the $\alpha$ phase are taken to be on the tetrahedral $d$ sites.) The upper-frequency modes, however, are spread over a broad range of energies compared to wurtzite. For the density-of-states calculation we have used a 5-$cm^{-1}$ resolution. However, for the ir and Raman calculations in the $\alpha$ phase we have used a 15-$cm^{-1}$ resolution to enable a better comparison with experiment. As can be seen in the figure, the calculated $\alpha$-phase infrared and Raman spectra are very different from the wurtzite spectra, since there are no selection rules to pick out particular modes. The spectra are therefore rather broad, with features which reflect the density of states. Note, however, that there are pronounced differences in couplings of modes in different frequency ranges, so that peaks in the different spectra do not precisely coincide with each other or with peaks in the density of states. For example, the upper peak in the ir spectrum is calculated to be at a higher frequency than that for the Raman spectra. This type of shift appears to occur in the experiments, although the relative movements are opposite to those given by our simple-coupling model. Note, however, that the lower-frequency Raman peak is calculated to occur at higher frequency than the corresponding density-of-states peak, while the infrared lower peak occurs at about the same place as that in the density of states. This aspect of the calculation does appear to bear some resemblance to the experimental results.

Figure 3 shows the contributions from each of the terms in Eq. (5) to the Raman scattering for "perfect" $\alpha$-phase AgI, i.e., Ag on the 12 $d$ sites with no static displacements. The resolution is still 5 $cm^{-1}$. The spectra for each term are broad, reflecting the intrinsically disordered nature of the $\alpha$ phase. This effectively destroys the $k \approx 0$ selection rules associated with Raman scattering in ordered crystals.

The low-frequency behavior of the experimental spectra presents some special issues.[20] By hydrodynamic arguments it can be shown that the density of phonon states should vary as $\omega^2$ at low frequency. Also, since a uniform translation does not change the polarizability, the first-order Raman matrix element for long-wavelength modes is expected to vanish as $\omega^2$ when $\omega$ tends to zero. Thus, for first-order scattering from long-wavelength modes, the reduced Raman spectrum should vanish as $\omega^4$, and the directly measured intensity should vanish as $\omega^2$ when $\omega$ tends to zero. The experimental spectra do not accord with this.[5] To investigate the low-frequency behavior, we have calculated densities of states and reduced Raman spectra at high resolution averaged over several larger models ($\sim 2000$ atoms) of $\alpha$-AgI. The ratio of the reduced spectrum to the density of states gives the matrix-element effect. In the range 7–25 $cm^{-1}$ the matrix

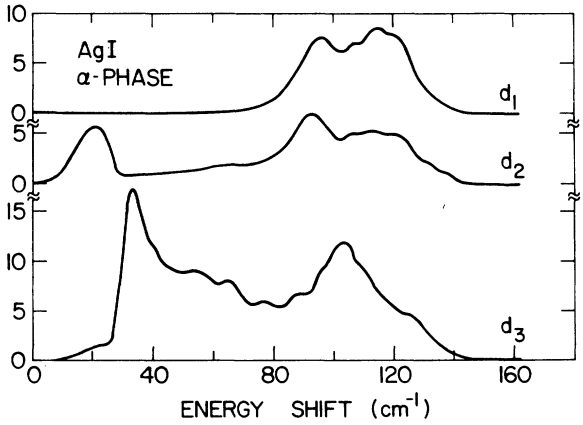


FIG. 3. Contributions to the Raman intensity from Eq. (5) for perfect $\alpha$-phase AgI.

element varies approximately as $\omega$ rather than $\omega^2$. (In the range 7–13 $cm^{-1}$ the calculated density of states does vary approximately as $\omega^2$.) We conclude from this that even in the harmonic approximation, the matrix-element effect for first-order scattering in disordered $\alpha$-phase AgI does not attain the limiting hydrodynamic behavior until frequencies lower than those accessible to our calculations. At very low frequencies, however, the diffusive motions neglected in our calculations are expected to dominate the experimental behavior.

## IV. TREATMENT OF DEFECT SITES

The preceding analysis shows that the intrinsic disorder of $\alpha$-phase AgI can explain many aspects of the spectra. However, it is also clear that deviations from the ideal tetrahedral positions occur, at least to some extent.[7,8] We take these deviations into account, in a rather simple way, and find that the results for the $\alpha$ phase are changed only a small amount. One would expect this, since the deviations cause only a small amount of extra disorder in an already disordered system. However, in the wurtzite phase of AgI, deviations from the ideal structure play a more important role in changing the spectra, because spectral response is added where there is none for the ideal case.

Consider the experimental spectra of wurtzite AgI at temperatures just below the transition to the $\alpha$ phase (see the left side of Fig. 4). The features associated with the normal wurtzite selection rules are discernible, notably the $E_2$ mode near 17 $cm^{-1}$ and a strong response near 106 $cm^{-1}$ from the $A_1$ (TO) and $E_1$ (TO) modes. (The LO modes and the high-frequency $E_2$ mode are not observable above −68 and −196°C, respectively.[11,21]) However, as can be seen, there is a great deal of intensity in a spectral region not associated with allowed one-phonon transitions in the usual wurtzite structure. There are two kinds of effects which might explain this: (a) disorder scattering from harmonic motion about fixed, or essentially fixed, deviations from the ideal positions and (b) "true" anharmonic effects where the time scales for large displacements and for motions about displaced positions cannot be separated, leading to a breakdown of the phonon description of the motion in any frequency regime. Effects of type (b) could be studied by molecular dynamics or by a direct attack on the nonlinear equations. This is something which will not be attempted in the present paper. We can, however, examine type (a) effects with ordinary lattice dynamics.

In order to consider defect scattering, we need to make assumptions about the kinds of defects and the forces and couplings to light associated with defect

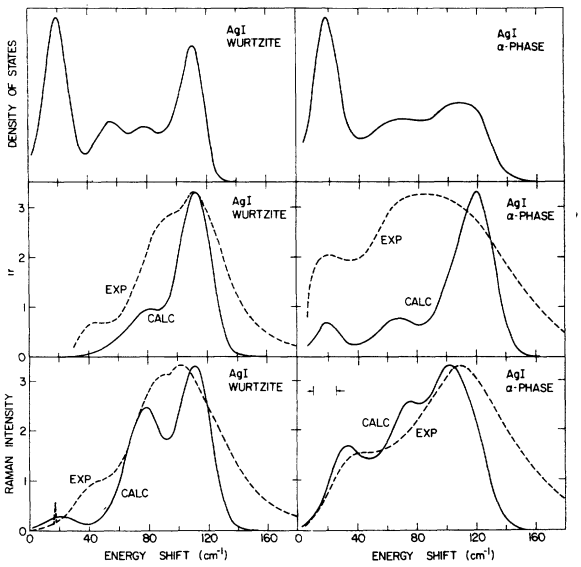


FIG. 4. Same results as in Fig. 2 but for the defect calculation, as described in the text. The calculated curves are solid lines, the experimental results dashed. The resolution for the calculation is 15 $cm^{-1}$ throughout.

sites. As mentioned, for the $\alpha$-phase AgI, there is some evidence for deviations[7,8] from the 12 $d$ sites. For wurtzite AgI, the evidence regarding the deviations from tetrahedral positions is controversial.[9,10] For both systems the problems in characterizing defects and their optical and dynamical properties compound the uncertainties associated with the harmonic approximation. Thus, we would like to make it clear that the calculations of this section should not be regarded as necessarily describing the large-scale motions in AgI more accurately than the basic calculations of Sec. III. Rather, they illustrate a class of effects which can explain further aspects of the observed spectra.

For $\alpha$-phase AgI we take each $Ag^+$ ion to have a small displacement from its $d$ site toward one of the four neighboring $d$ sites.[7] For wurtzite AgI we take each $Ag^+$ ion to have a small displacement in the direction of one of the four faces of the tetrahedra of surrounding $I^-$ ions. This is what is observed in CuI,[10] and perhaps in AgI.[9] Then in both of these structures the $Ag^+$ ion is displaced away from one of its four surrounding $I^-$ ions. We take this displacement to be 0.1 of the normal bond length in the material and reduce the force constants and polarizabilities associated with the stretched bond to 0.4 of the values used for the compressed bonds.

In the left side of Fig. 4 we show the density of states and spectra for wurtzite AgI with all the $Ag^+$ ions in defect positions. Experimental spectra are also indicated. It is seen that the defects give rise

to a new peak at 80 $cm^{-1}$ in the density of states and corresponding peaks in the infrared and Raman spectra. There is a considerable increase in the overall Raman intensity, largely because purely polarized scattering [the $d_3$ term in Eq. (5)], forbidden for the ideal tetrahedral sites, becomes allowed in the defect configurations. Thus, spectral response in the region of the acoustic branch can be seen. This is a general result that will occur independent of the detailed nature of the defect. In the right side of Fig. 4 we show similar results for $\alpha$-phase AgI with defects. Here again a special defect related peak in the density of states appears at 80 $cm^{-1}$, but it is less pronounced because of the broad spectra due to the disorder already present in the $\alpha$ phase. In Fig. 4, as in Fig. 2, twice the weight is given to the polarized spectra ($d_3$ term) as the depolarized spectra.

This model study of deviations from the ideal structure shows that defects with appropriate coupling could be called upon to explain the features of the spectrum of wurtzite AgI near the transition to the $\alpha$ phase. However, discerning the relative roles of defects and true anharmonic effects on the wurtzite-phase spectrum will require further experimental and theoretical study. In the $\alpha$ phase the dominant effects are not defects, but rather the intrinsic disorder in the statistical occupation of the 12 $d$ sites. However, some broadening and other features due to defects can be expected.

## V. DISCUSSION

The spirit of this work has been to strip away all complications from the description of the dynamics and the optical couplings, so that we could treat the effects of static disorder on the density of states and the spectra. Once the possible effects of disorder have been elucidated, we may then get a feeling for those aspects of the spectra which require more detailed consideration of the true motions, including anharmonic coupling and diffusion-related effects.

Our results show that for $\alpha$-phase AgI the principal features of the experimentally observed Raman[5,14,16,17,21,22] and infrared[23,24] spectra can be understood in terms of the intrinsic disorder of this material. In particular, a broad spectrum which peaks at about 106 $cm^{-1}$ and has a feature at $\approx$30 $cm^{-1}$ reflecting the presence of a large number of TA-like modes is expected and seen in Raman scattering. The addition of defects in the $\alpha$ phase makes relatively little difference in our calculated results, as one would guess, since the selection rules are already broken. The calculated low-frequency conductivity in the $\alpha$ phase, as taken from the ir response in Figs. 2 and 4, is considerably below the dc conductivity, which varies from 1.3 $(\Omega\,cm)^{-1}$ at $T_c$ to 2.6 $(\Omega\,cm)^{-1}$ at the melting temperature. The calculated curves in these figures have been normalized so that they peak at 3.3 $(\Omega\,cm)^{-1}$ to agree with the experimental ir results. If we normalized the calculated curves by demanding that the integral under the curve be the same as the experimental results (the sum rule[1,3,4]), the calculated results at low frequencies would still be considerably below the measured dc values.[5,21,23] The fact that the measured dc conductivity, which is due entirely to diffusion, decreases between 0 and 1 or 2 $cm^{-1}$ and then increases in the manner given by our phonon calculation can be taken as confirming our assumption that the effects of diffusion are dominant only at the lowest frequencies in a $\alpha$-phase AgI.

For the wurtzite phase of AgI, our results are much more tentative. We have investigated some of the effects of static defects on the spectra. The defects were taken as displaced $Ag^+$ ions. These defects, or other types of static disorder, might explain the spectral changes observed as temperature is increased toward the phase transition at 147°C, above which the $\alpha$ phase exists. The defects allow spectral intensity to appear with features of the phonon density of states as well as special defect related peaks as discussed in the paper. However, both in this phase and in the $\alpha$ phase some of the spectra could be second order in nature.[25]

There have been several papers[24,26-30] that treat the dynamics of the $\alpha$-phase AgI in terms of a single dampled harmonic oscillator which can change over to obey a diffusion equation at low frequencies in order to get a nonzero dc conductivity at $\omega = 0$. This changeover has been described by a simple phenomenological model[27] which appears to reproduce various features of the experiments. However, detailed calculations[24,30] for a particle diffusing in a periodic potential contradict the results of the simple model and indicate that cooperative effects must be important for the dynamics of the diffusion.

Our work clearly does not describe the diffusive motion in AgI.[31] However, we can conclude that even the oscillatory aspect of the motion is not simple and that better treatments of both oscillatory and diffusive motion will be required to describe the overall spectra in detail.

†Work supported in part by the National Science Foundation.

*Present address: General Electric Research and Development Center, Schenectady, N.Y. 12301.

[1]For a summary of the field, see (a) *Fast Ion Transport Solids, Solid State Batteries and Devices*, edited by W. Von Gool (North-Holland, Amsterdam, 1973); (b) *Superionic Conductors*, edited by G. D. Mahan and W. L. Roth (Plenum, New York, 1976); (c) K. Funke, Prog. Solid State Chem. 11, 345 (1976).

[2]R. Alben and G. Burns, Bull. Am. Phys. Soc. 22, 442 (1977).

[3]L. W. Strock, Z. Phys. Chem. B 25, 411 (1934); 31, 132 (1936); S. Hoshimo, J. Phys. Soc. Jpn. 12, 315 (1957).

[4]For example, see S. Geller, in Ref. 1(a), p. 607.

[5]G. Burns, F. H. Dacol, and M. W. Shafer, Solid State Commun. 19, 291 (1976).

[6]R. J. Cava and B. J. Wuench, in Ref. 1(b), p. 217.

[7]J. B. Boyce, T. M. Hayes, W. Stutius, and J. C. Mikkelsen, Jr. (unpublished).

[8]F. Rerdinger (private communication).

[9]L. Helmholtz, J. Chem. Phys. 3, 740 (1935); K. W. Leiser, Z. Phys. Chem. (Frankfurt am Main) 9, 216 (1956); 9, 302 (1956); G. Burley, J. Chem. Phys. 38, 2807 (1963); B. R. Lawn, Acta Cryst. 17, 1341 (1964). The last paper discusses the anomalous properties of the wurtzite phase, such as a negative thermal expansion, and is a nice summary.

[10]S. Miyake, S. Hoshino, and T. Takenaka, J. Phys. Soc. Jpn. 7, 19 (1952).

[11]G. L. Bottger and C. V. Damsgard, J. Chem. Phys. 53, 1215 (1972).

[12]M. Born, Ann. Phys. (Leipzig) 44, 605 (1914); M. Born and K. Huang, *Dynamical Theory of Crystal Lattices* (Clarendon, Oxford, 1954).

[13]D. E. Beeman and R. Alben, Adv. Phys. (to be published).

[14]W. Bührer and P. Brüesch, Solid State Commun. 16, 155 (1975).

[15]R. Alben, D. Weaire, J. E. Smith, Jr., and M. H. Broadsky, Phys. Rev. B 11, 2271 (1975).

[16]R. C. Hanson, T. A. Fjeldly, and H. D. Hockheimer, Phys. Status Solidi 70, 567 (1975).

[17]M. J. Delaney and S. Ushioda, Solid State Commun. 19, 297 (1976).

[18]M. H. Broadksy, in *Topics in Applied Physics*, edited by M. Cardona (Springer-Verlag, Berlin, 1975), p. 205.

[19]G. L. Bottger and A. L. Geddes, J. Chem. Phys. 46, 3000 (1967).

[20]See Ref. 17, pp. 212–215, for a discussion and references about this point.

[21]G. Burns, F. H. Dacol, and M. W. Shafer, Phys. Rev. B (to be published).

[22]R. T. Harley, W. Hayes, A. J. Rushworth, and J. F. Tyan, in *Light Scattering in Solids*, edited by M. Balkanski, R. C. C. Leite, and S. P. S. Porto (Flammarion, Paris, 1976), p. 346.

[23](a) K. Funke and A. Jost, Nachr. Akad. Wiss. Goettingen 15, 137 (1969); (b) W. Jost, K. Funke, and A. Jost, Z. Naturforsch. 25a, 983 (1970); (c) K. Funke and A. Jost, Ber. Bunsenges. Phys. Chem. 75, 436 (1971).

[24]P. Brüesch, S. Strässler, and H. R. Zeller, Phys. Status Solidi A 31, 217 (1975).

[25]M. J. Delaney and S. Ushioda, Bull. Am. Phys. Soc. 22, 365 (1977).

[26]M. J. Rice and W. L. Roth, J. Solid State Chem. 4, 294 (1972).

[27]B. A. Huberman and P. N. Sen, Phys. Rev. Lett. 33, 1379 (1974); P. N. Sen and B. A. Huberman, *ibid.* 34, 1059 (1975).

[28]W. J. Pardee and G. D. Mahan, J. Solid State Chem. 15, 310 (1975).

[29]P. Fulde, L. Pietronero, W. R. Schneider, and S. Strassler, Phys. Rev. Lett. 35, 1776 (1975).

[30]P. Brüesch, L. Pietronero, S. Strässler, and H. R. Zeller, Phys. Rev. B (to be published).

[31]K. Funke and his collaborators have published several papers in this area. The work is conveniently reviewed in Ref. 1(c).